Diffuse x-ray reflection from multilayers with stepped interfaces

V. Holý

Laboratory of Thin Films and Nanostructures, Faculty of Science, Kotlářská 2, 611 37 Brno, Czech Republic

C. Giannini and L. Tapfer

Centro Nazionale Ricerca e Sviluppo Materiali (PASTIS-CNRSM), Strada Statale 7 Appia km. 712, I-72100 Brindisi, Italy

T. Marschner and W. Stolz

Wissenschaftliches Zentrum für Materialwissenschaften und Fachbereich Physik, Philipps-Universität, D-35032 Marburg, Germany

Diffuse x-ray reflection from a multilayer with stepped interfaces has been investigated theoretically and experimentally. The statistical description of the stepped interfaces has been based on the theory of random processes. Diffuse x-ray scattering from those interfaces has been calculated using the distorted-wave Born approximation. The theory has been used for an analysis of the intensity distributions measured on a GaAs/(GaIn)As/GaAs/Ga(PAs) strained-layer superlattice grown on a miscut substrate. From the measurements, the mean size of the interface terraces and their orientations could be determined. [S0163-1829(97)02612-X]

I. INTRODUCTION

Nonspecular (diffuse) x-ray reflectivity is a very powerful tool for investigating the morphology of surfaces and interfaces of multilayers. It has been demonstrated previously[1–8] that the distribution of the diffusely scattered intensity in reciprocal plane is connected with the correlation function of the interface roughness. In addition, the replication of the interface roughness (i.e., the correlations of the roughness profiles of different interfaces in the multilayer) substantially influences the diffuse x-ray scattering. The theoretical description of the reciprocal space distribution of the scattered intensity was based on the distorted-wave Born approximation (DWBA),[1,3,7,9] which includes also the dynamical effects accompanying the diffuse scattering from rough interfaces.

In most papers, the experimental data have been analyzed assuming the roughness correlation function following from the fractal correlation model.[1,4,6] The basic properties of this model can be derived if the growth of the surface is modeled by the Edwards-Wilkinson-Langevin equation[10] or by the more general Kardar-Parisi-Zhang equation.[11]

Within the fractal model, due to the self-affinity of the fractal roughness profile, the calculated intensity distribution exhibits no subsidiary maxima in reciprocal plane in the direction parallel to the sample surface. However, in recent papers concerning strained crystalline multilayers [GaAs/AlAs (Refs. 12–14) and SiGe/Si (Refs. 15–20)] and crystalline surfaces[21–23] another type of the interface roughness has been reported. The distribution of the diffusely scattered intensity in reciprocal plane was explained by means of a terraced structure. The angle between the terrace levels and the mean interface could be deduced from the asymmetry of the intensity distribution in reciprocal plane. If the dispersion of the terrace widths was not too large, subsidiary intensity maxima appeared in reciprocal plane in the direction parallel to the surface. Then, the mean terrace size was estimated

from the separation of these lateral intensity satellites.

Theoretical analysis of diffuse x-ray scattering from terraced structures was based on the domain-matrix method[22] or on a simple model describing the faceted surface as a locally flat and randomly disoriented surface.[24] The concept of the terraced surfaces has often been used for the analysis of RHEED data[25] and several types of terraced structures have been discussed using the approach of stationary random processes. Using this method and the kinematical scattering theory, the intensity scattered by a terraced surface was obtained in the form of the Fourier transformation of the pair correlation function of the surface. The method has been used for the analysis of x-ray diffuse scattering from single terraced surfaces[21] and from multilayers,[15,16] in the latter case, however, no quantitative agreement of measured data with the theory was achieved.

The goal of this paper is to describe the diffuse x-ray reflection from multilayers with terraced interfaces using the DWBA method assuming the correlation properties of the terraced structure.[25] We discuss the influence of the orientation of the terraces on the reciprocal space intensity distribution. We also take into account the partial correlation of the positions of the terrace edges in different interfaces.

In the first part of the paper, we determine the correlation function of the terraced interface on the basis of the theory published previously[25] and we postulate a suitable description of the replication of the terrace structure. Then, we use this correlation function for the calculation of the intensity distribution in reciprocal plane. In the final part, the theoretical results will be compared numerically with experimental data obtained on GaAs/Ga$_{1-x}$In$_x$As/GaPAs multilayers.

II. DESCRIPTION OF A STEPPED SURFACE

The description of a stepped surface will be based on the approach of stationary random processes.[25] Let us assume a surface consisting of an infinite number of parallel terraces
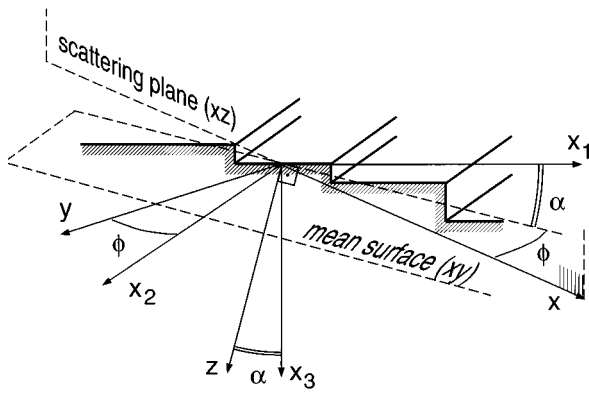
FIG. 1. Sketch of the coordinate systems. The coordinate axes x_1, x_2, x_3 are parallel to the main crystallographic axes of the sample, the axes x, y, z are defined by the mean sample surface and by the scattering plane. α is the angle between the terrace levels and the mean surface, ϕ is the azimuthal angle of the scattering plane.

creating a random descending staircase. We introduce the coordinates x_1, x_2, x_3 parallel and perpendicular to the terrace levels, according to Fig. 1. The mean surface is inclined with respect to the terraces by small angle $\alpha \approx \langle h \rangle / \langle L \rangle$, where $\langle h \rangle$ and $\langle L \rangle$ are the mean height of the terrace steps and the mean width of the terraces, respectively. It is reasonable to assume that the terrace levels are parallel to crystallographic planes with low Miller indices, therefore α equals the crystallographic misorientation of the surface.

We introduce the pair correlation function $C(x_1, x_2, x_3)$ of the surface. It equals the probability per unit height x_3 that two surface atoms with lateral coordinates $(0,0)$ and (x_1, x_2) have the difference x_3 of their vertical coordinates.

At first, let us consider two surface atoms, the first one ($A1$) in the origin $(0,0,0)$ and the second ($A2$) in some point $(x_1 > 0, 0, x_3)$. If these atoms are separated by n steps, the probability per unit height x_3 of finding this configuration is[25]

$$w_n(x_1, x_3) = \int_0^\infty dL_0 \int_0^\infty dL_1 \cdots \int_0^\infty dL_n P_0(L_0)$$
$$\times P(L_1) \cdots P(L_{n-1}) P_f(L_n)$$
$$\times \int_{-\infty}^\infty dh_1 \cdots \int_{-\infty}^\infty dh_n H(h_1) \cdots H(h_n)$$
$$\times \delta \left(x_1 - \sum_{j=0}^n L_j \right) \delta \left(x_3 - \sum_{j=1}^n h_j \right), \quad (1)$$

where $L_0, \ldots, L_n$ are the width of the terraces between the chosen surface atoms and $h_1, \ldots, h_n$ are the heights of the steps. $P(L_j)$ is the probability per unit length of a terrace of width L_j, $H(h_j)$ is the probability per unit height of finding a step of height h_j between two terraces. The function $P_0(L_0)$ is the probability per unit length that there is the first step in the distance L_0 from the atom $A1$ and $P_f(L_n)$ means the probability that the atom $A2$ is at the distance L_n from the last (nth) step.

The pair correlation function of the atoms $A1$ and $A2$ is then

$$C(x_1 > 0, 0, x_3) = P_{0f}(x_1) \delta(x_3) + \sum_{n=1}^\infty w_n(x_1, x_3), \quad (2)$$

where $P_{0f}(x_1)$ is the probability of finding the atom $A2$ at the same terrace. Since $C(x_1, 0, x_3) = C(-x_1, 0, -x_3)$ an analogous formula for $C(x_1 < 0, 0, x_3)$ can simply be obtained,[25]

$$P_0(L) = \frac{1}{\langle L \rangle} \int_L^\infty dl P(l), \quad P_f(L) = \int_L^\infty dl P(l), \quad (3)$$

and

$$P_{0f}(L) = \frac{1}{\langle L \rangle} \int_L^\infty dl (l - L) P(l). \quad (4)$$

Then, using the Fourier transforms (FT) of the probability distributions

$$P^{\mathrm{FT}}(q) = \int_0^\infty dL P(L) e^{iqL}, \quad H^{\mathrm{FT}}(q) = \int_{-\infty}^\infty dh H(h) e^{ihq}$$

we obtain the two-dimensional Fourier transformation of the correlation function in the form

$$C^{\mathrm{FT2}}(q_1, q_3) = \int_{-\infty}^\infty dx_1 \int_{-\infty}^\infty dx_3 C(x_1, 0, x_3) e^{i(q_1 x_1 + q_3 x_3)}$$
$$= 2 \mathrm{Re} \left[\frac{1 - P^{\mathrm{FT}}(q_1)}{q_1^2 \langle L \rangle} \left(1 - [1 - P^{\mathrm{FT}}(q_1)] \right. \right.$$
$$\left. \left. \times \sum_{n=1}^\infty [P^{\mathrm{FT}}(q_1)]^{n-1} [H^{\mathrm{FT}}(q_3)]^n \right) \right]. \quad (5)$$

If $q_1 \neq 0$ or $q_3 \neq 0$, the infinite sum in the last formula converges and we obtain finally

$$C^{\mathrm{FT2}}(q_1, q_3) = \frac{2}{q_1^2 \langle L \rangle} \mathrm{Re} \left[\frac{[1 - P^{\mathrm{FT}}(q_1)][1 - H^{\mathrm{FT}}(q_3)]}{1 - P^{\mathrm{FT}}(q_1) H^{\mathrm{FT}}(q_3)} \right]. \quad (6)$$

Now, we postulate the form of the general correlation function $C(x_1, x_2, x_3)$, i.e., we do not assume that the atoms $A1$ and $A2$ have the same coordinate x_2. We assume that the terraced surface is divided into domains of mean length $\langle D \rangle$ in the x_2 direction. The terrace length D in this direction is random as well, having the probability per unit length $R(D)$. Within one domain, the shape of the terraces does not depend on x_2, and, in two different domains, the positions of the terraces are statistically independent. The correlation function can be postulated in the following approximate form:

$$C(x_1, x_2, x_3) = C(x_1, 0, x_3) R_{0f}(x_2), \quad (7)$$

where $R_{0f}(x_2)$ is the probability that both surface atoms lie in the same domain. Similarly to P_{0f}, this probability is

$$R_{0f}(|D|) = \frac{1}{\langle D \rangle} \int_{|D|}^\infty dl (l - |D|) R(l). $$

Thus, the (three-dimensional) Fourier transform of the pair correlation function is

$$C^{\mathrm{FT}}(\mathbf{q}) = \frac{2}{q_2^2 \langle D \rangle} \mathrm{Re}[1 - R^{\mathrm{FT}}(q_2)] C^{\mathrm{FT2}}(q_1, q_3). \quad (8)$$

We will assume that the terrace widths L are distributed according to the gamma distribution of the order M:[25]

$$P(L) = \frac{1}{\Gamma(M)} \left(\frac{M}{\langle L \rangle} \right)^M \exp\left(-\frac{M}{\langle L \rangle} L \right) L^{M-1}. \quad (9)$$

The dispersion of this distribution is

$$\sigma_L^2 = \frac{\langle L \rangle^2}{M}$$

and its Fourier transformation (characteristic function)

$$P^{\mathrm{FT}}(q) = \left(1 - \frac{iq \langle L \rangle}{M} \right)^{-M}.$$

For $M = 1$ we obtain the geometric (exponential) distribution and in the limit $M \to \infty$ we obtain

$$P^{\mathrm{FT}}(q) \to e^{iq \langle L \rangle}.$$

The statistical distribution of the terrace lengths D will be given by the gamma distribution as well, having the order M'. The random step heights h will be distributed normally with the mean value $\langle h \rangle = \langle L \rangle \alpha$ and the dispersion σ_h^2.

III. DIFFUSE X-RAY SCATTERING FROM MULTILAYERS WITH STEPPED INTERFACES

Let us deal with a multilayer with stepped interfaces whose statistical properties have been described in the preceding section. The multilayer consists of N layers and interfaces $j = 0, 1, \ldots, N$. The interface $j = 0$ is the free surface, $j = N$ is the substrate surface. The interface j lies between the layers j and $j + 1$.

The intensity of the scattered radiation can be expressed as a function of the momentum transfer vector in vacuum,

$$\mathbf{Q} = \mathbf{K}_2 - \mathbf{K}_1, \quad (10)$$

where $\mathbf{K}_1$ and $\mathbf{K}_2$ are the (vacuum) wave vectors of the primary and scattered beams, respectively. The wave vector $\mathbf{K}_1$ and the normal to the mean sample surface define the scattering plane. We introduce the orthogonal coordinates x, y, z so that z is parallel to the inward normal to the mean surface and x lies in the scattering plane. The mean interface j lies in the depth $\langle z_j \rangle$ below the surface ($\langle z_0 \rangle = 0$). In the following, $\mathbf{x} = (x, y, 0)$ denotes the in-plane component of the position vector $\mathbf{r}$.

The orientation of the axes x, y, z with respect to the crystallographic axes x_1, x_2, x_3 is defined by the angles α and ϕ, where ϕ is the azimuth angle between the scattering plane and the direction normal to the terrace edges. If the misorientation angle α is small enough, the following transformation relations are valid (see Fig. 1):

$$x_1 = x \cos\phi - y \sin\phi - z \alpha,$$

$$x_2 = x \sin\phi + y \cos\phi, \quad (11)$$

$$x_3 = (x \cos\phi - y \sin\phi) \alpha + z.$$

In reciprocal space, similar formulas can be derived for the transformation of the vector (q_1, q_2, q_3) into (q_x, q_y, q_z).

The scattering process is entirely described by the wave equation

$$(\triangle + K^2) E(\mathbf{r}) = V(\mathbf{r}) E(\mathbf{r}). \quad (12)$$

We limit ourselves to the scalar electric field $E(\mathbf{r})$, i.e., we do not take into account the polarization effects. $K = 2\pi/\lambda$ is the vacuum wave vector,

$$V(\mathbf{r}) = K^2[1 - n(\mathbf{r})]$$

is the scattering potential, and $n(\mathbf{r})$ is the refractive index of the sample.

We solve the wave equation (12) by means of the DWBA method.[1,3] Within this approach, the scattering potential is divided into two parts $V = V^{(0)} + V^{(1)}$, where the undisturbed part $V^{(0)}$ corresponds to the semi-infinite substrate with flat surface and the refractive index $n^{(0)}$. $V^{(1)}$ is the disturbance due to the multilayer structure and the interface roughness. The DWBA method can also be used in another way, assuming the undisturbed system being a multilayer with flat interfaces.[3,5,7] Our choice of the undisturbed system means that we neglect the influence of the coherent reflection from the multilayer interfaces on the diffuse scattering. Thus, we neglect the dynamical Bragg-like peaks in the distribution of the diffusely scattered intensity. As we show later, these peaks were not present in the measured data. Most likely, the large interface roughness in the sample suppressed both the coherent reflectivity and the dynamical features in the diffuse scattering. In this case, the choice of the undisturbed system with flat interfaces[3] is not suitable.

In contrast to the usual Born approximation, the matrix element of the scattering matrix due to the disturbance is expressed on the basis of two independent eigenstates $|1\rangle$ and $|2\rangle$ of the undisturbed potential $V^{(0)}$. These eigenstates are plane waves, whose wave vectors $\mathbf{k}_1$ and $\mathbf{k}_2$ are connected to the vacuum wave vectors $\mathbf{K}_{1,2}$ by the refraction law

$$\mathbf{k}_{s\parallel} = \mathbf{K}_{s\parallel}, \quad k_{sz} = \pm \sqrt{(n^{(0)}K)^2 - |\mathbf{K}_{s\parallel}|^2}, \quad s = 1, 2, \quad (13)$$

where the upper sign belongs to the state $|1\rangle$. The amplitudes of these eigenstates equal the complex Fresnel transmittivity coefficients $T_{1,2}$ corresponding to the incident waves $\mathbf{K}_1$ and $-\mathbf{K}_2$, respectively. The element of the scattering matrix is therefore[1]

$$\mathcal{V}^{(1)} = \langle 2|V^{(1)}|1 \rangle = T_1 T_2 \int d^3\mathbf{r} V^{(1)}(\mathbf{r}) e^{i\mathbf{q} \cdot \mathbf{r}},$$

where $\mathbf{q} = \mathbf{k}_2 - \mathbf{k}_1$ is the momentum transfer vector inside the undisturbed medium. Its in-plane component $\mathbf{q}_\parallel$ equals the in-plane component $\mathbf{Q}_\parallel$ of the vacuum momentum transfer; the vertical component q_z is different, due to the refraction law (13). The imaginary part of q_z expresses the absorption.

We denote $n_j = 1 - \delta_j$ the refraction index of the jth layer; $n_S = 1 - \delta_S$ is the refraction index of the substrate. The pro-

file of the jth interface is described by a random function $U_j(\mathbf{x}) = z_j(\mathbf{x}) - \langle z_j \rangle$. The matrix element is then

$$\mathcal{V}^{(1)} = 2K^2 T_1 T_2 \int d^2\mathbf{x} e^{i\mathbf{Q}_\parallel \cdot \mathbf{x}}$$

$$\times \sum_{j=1}^{N} (\delta_j - \delta_S) \int_{\langle z_{j-1} \rangle + U_{j-1}}^{\langle z_j \rangle + U_j} dz e^{iq_z z}. \quad (14)$$

After simple algebra we obtain

$$\mathcal{V}^{(1)} = \frac{2K^2 T_1 T_2}{iq_z} \sum_{j=0}^{N} (\delta_j - \delta_{j+1}) e^{iq_z \langle z_j \rangle} \int d^2\mathbf{x} e^{i\mathbf{Q}_\parallel \cdot \mathbf{x}} e^{iq_z U_j(\mathbf{x})},$$

$$(15)$$

where we set $\delta_0 = 0$.

From the element of the scattering matrix, the differential cross section of the scattering into an elementary solid angle $d\Omega$ can be calculated using the following simple formula:[1]

$$\frac{d\sigma}{d\Omega} = \frac{\langle |\mathcal{V}^{(0)} + \mathcal{V}^{(1)}|^2 \rangle}{16\pi^2}$$

$$= \frac{1}{16\pi^2}[|\mathcal{V}^{(0)}|^2 + 2\mathrm{Re}(\mathcal{V}^{(0)}\langle \mathcal{V}^{(1)} \rangle^*) + \langle |\mathcal{V}^{(1)}|^2 \rangle],$$

$$(16)$$

where $\mathcal{V}^{(0)} = \langle 2|V^{(0)}|10 \rangle$ is the element of the undistorted scattering matrix and $|10\rangle$ is the vacuum (incident) wave giving rise to the undistorted eigenstate $|1\rangle$. Since the sample is assumed to be statistically homogeneous, $\mathcal{V}^{(0)}$ and $\langle \mathcal{V}^{(1)} \rangle$ are proportional to $\delta(\mathbf{Q}_\parallel)$. Therefore, the first two terms on the right-hand side of Eq. (16) only contribute to the coherent (specularly reflected) wave.

In the following, we limit ourselves to the incoherent part of the cross section. This part describes the wave diffusely scattered from the interface roughness and is given by the matrix element $\mathcal{V}^{(1)}$

$$\frac{d\sigma_D}{d\Omega} = \frac{\langle |\mathcal{V}^{(1)}|^2 \rangle}{16\pi^2}. \quad (17)$$

From Eqs. (15) and (17) we obtain

$$\frac{d\sigma_D}{d\Omega} = \frac{SK^4}{4\pi^2} \frac{|T_1 T_2|^2}{|q_z|^2} \sum_{j,k=0}^{N} (\delta_{j+1} - \delta_j)$$

$$\times (\delta_{k+1} - \delta_k)^* e^{i(q_z \langle z_j \rangle - q_z^* \langle z_k \rangle)} \int_S d^2\mathbf{x} e^{i\mathbf{Q}_\parallel \cdot \mathbf{x}} Z_{jk}(\mathbf{x}),$$

$$(18)$$

where S is the sample surface irradiated by the primary wave, and

$$Z_{jk}(\mathbf{x} - \mathbf{x}') = \langle \exp\{i[q_z U_j(\mathbf{x}) - q_z^* U_k(\mathbf{x}')]\} \rangle. \quad (19)$$

If $j = k$, this function is connected to the pair correlation function of the interface defined in the preceding section by

$$Z_{jj}(\mathbf{x} - \mathbf{x}') = \int_{-\infty}^{\infty} d(z - z') C(x - x', y - y', z - z')$$

$$\times e^{i(z - z')\mathrm{Re}(q_z)}, \quad (20)$$

where we have neglected the absorption of x rays within the terrace steps. For the sake of simplicity, we will assume that the pair correlation function C is the same for all interfaces, and thus Z_{jj} does not depend on j.

If $j = k$, the terrace replication must be taken into account. It has been reported previously[17,18] that the direction of maximum replication could be different from the growth direction. We describe the replication direction by a unit vector $\mathbf{b}$ and the function Z_{jk} can be assumed in the form

$$Z_{jk}(\mathbf{x} - \mathbf{x}') = \{Z_{jj}[\mathbf{x} - \mathbf{x}' - \mathbf{b}_\parallel(\langle z_j \rangle - \langle z_k \rangle)] - |\mathcal{E}|^2\}$$

$$\times \exp\left(-\frac{|\langle z_j \rangle - \langle z_k \rangle|}{\Lambda_\perp}\right) + |\mathcal{E}|^2. \quad (21)$$

Here $\mathbf{b}_\parallel$ is the in-plane component of $\mathbf{b}$ determining the azimuthal direction of the maximum replication and the angle χ of $\mathbf{b}$ with the negative z axis. The exponential term shows that the replication of the steps could be only partial; $\Lambda_\perp$ is the replication length.[26] The term $\mathcal{E}$ is analogous to the static Debye-Waller factor

$$\mathcal{E} = \langle e^{iq_z U_j(\mathbf{x})} \rangle$$

that depends neither on the index j nor on $\mathbf{x}$. This term contributes to the specular reflectivity only and can be further omitted.

From Eqs. (21) and (18) we obtain the final formula for the diffuse part of the differential cross section,

$$\frac{d\sigma_D}{d\Omega} = \frac{SK^4}{4\pi^2} \frac{|T_1 T_2|^2}{|q_z|^2} |C^{\mathrm{FT}}(\mathrm{Re}(\mathbf{q}))|^2 \sum_{j,k=0}^{N} (\delta_{j+1} - \delta_j)$$

$$\times (\delta_{k+1} - \delta_k)^* \exp[i(q_z \langle z_j \rangle - q_z^* \langle z_k \rangle)]$$

$$\times \exp[i(\langle z_j \rangle - \langle z_k \rangle)(\mathbf{Q}_\parallel \cdot \mathbf{b}_\parallel)]$$

$$\times \exp\left(-\frac{|\langle z_j \rangle - \langle z_k \rangle|}{\Lambda_\perp}\right). \quad (22)$$

From the differential cross section, the intensity of the diffusely scattered radiation can be calculated integrating $d\sigma_D$ over the solid entrance angle of the detector slit and multiplying it by the intensity flux I_0/S_0 of the primary beam. In our further considerations, the aperture angle of the detector will be very large in the direction perpendicular to the scattering plane and its value $\Delta\theta$ in the scattering plane will be very small. Then, the scattered intensity is

$$I_D(Q_x, Q_z) = \frac{I_0}{S_0} \frac{\Delta\theta}{K} \int_{-\infty}^{\infty} dQ_y \frac{d\sigma_D}{d\Omega}. \quad (23)$$

From the last two formulas it follows that the scattered intensity is proportional to the ratio S/S_0 of the irradiated sample surface and the cross section of the primary beam. If only a part of the sample surface is irradiated, S depends on the angle of incidence of the primary beam. This fact causes

a certain asymmetry of the intensity distribution in reciprocal plane with respect to the Q_z axis.

The differential cross section $d\sigma_D$ can be expressed as a product of two terms. The first one $[C^{FT}(Re(\mathbf{q}))]$ mainly depends on $\mathbf{Q}_{\parallel}$. Thus, the lateral correlation properties of the interfaces (terrace size, its statistical distribution, etc.) can be obtained by investigating the intensity distribution along the Q_x axis. This fact is caused by the assumption that these properties are the same for all the interfaces. If the interfaces were not statistically equivalent, only some effective values of the terrace parameters could be determined from the measured intensity distribution.

The remaining part of the expression (22) for σ_D depends mainly on Q_z. Therefore, the replication of the terrace steps of different interfaces can be established from the Q_z dependence of the scattered intensity. If the interface profiles are replicated and the multilayer is periodical, periodical maxima on the Q_z dependence of the diffusely scattered intensity occur. If we neglect the refraction, the distance of these maxima is $2\pi/D$, where D is the multilayer period. This behavior of the diffuse scattering is analogous to the case of fractal interface roughness (resonant diffuse scattering maxima[3]). The width of these maxima in the Q_z direction is inversely proportional to $\Lambda_{\perp}$. In reciprocal plane, the maxima are elongated in a direction perpendicular to $\mathbf{b}$. Therefore, from the shape of these maxima, the direction of maximum replication can be found. In this paper, we will not deal with the replication of the stepped interfaces, which will be the subject of the next publication.

The behavior of the term $|C^{FT}(Re(\mathbf{q}))|^2$ in Eq. (22) is illustrated in Figs. 2, 3, and 4, where we have plotted the calculated intensity I_D diffusely scattered from a single stepped surface.

Figures 2(a)–2(c) show the function $I_D(Q_x,Q_z=const)$ calculated for different $\langle L \rangle$ [Fig. 2(a)], σ_L [Fig. 2(b)], and σ_h [Fig. 2(c)]. The curves exhibit periodical maxima (lateral satellites), having the distance $2\pi/\langle L \rangle$; the width of these maxima is inversely proportional to σ_L and σ_h. Therefore, from a single Q_x scan it is nearly impossible to determine both σ_L and σ_h.

In Figs. 3(a)–3(c), we demonstrate the dependence of the intensity distribution $I_D(Q_x,Q_z)$ on the angle α. It is obvious that the envelope curve of the satellite maxima is elongated in reciprocal plane in a direction parallel to the terraced levels, i.e., it is inclined by angle α with respect to the axis Q_z. However, the lateral satellites are always perpendicular to the *mean* surface.

In Fig. 4, the theoretical functions $I_D(Q_x,Q_z=const)$ are plotted for different azimuthal angles ϕ. If $\phi=0°$ the axis x_1 is parallel to x and the scattered intensity does not depend on the terrace lengths D. In the case $\phi=90°$, the axis x_2 is parallel to x and the intensity distribution is only influenced by the terrace lengths D and their statistical distribution $R(D)$. Then, no lateral satellites can be observed. In the intermediate case ($\phi=45°$) the distance of the lateral satellites is smaller by a factor of $\cos\phi$ and the satellites are broader.

IV. GROWTH PROCEDURES AND EXPERIMENTAL DETAILS

The sample investigated here was grown by metalorganic vapor phase epitaxy (MOVPE) in a commercial system (AIX
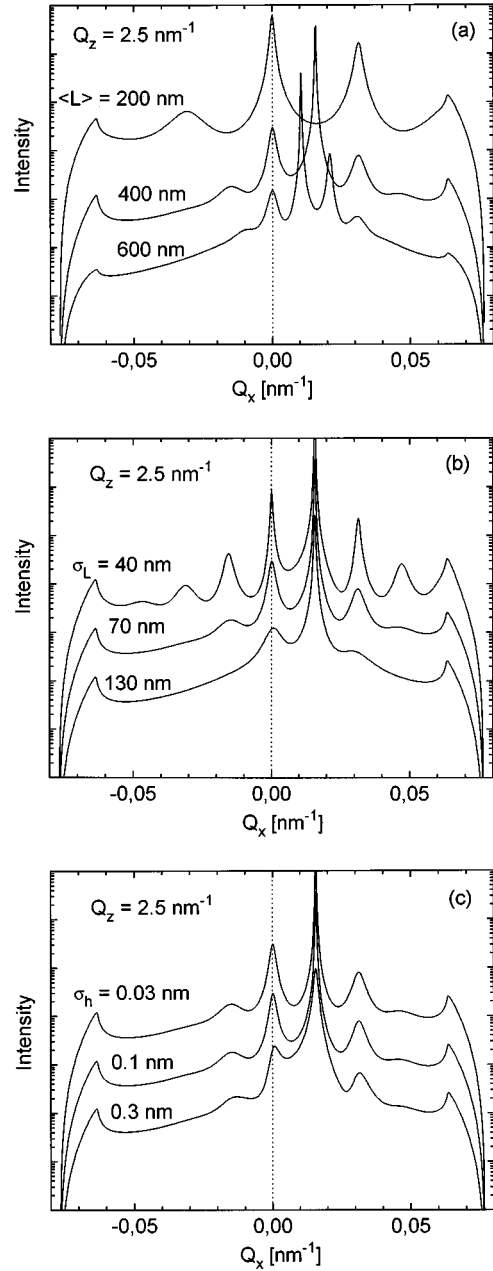

FIG. 2. The calculated dependence of the intensity diffusely scattered on Q_x from a single terraced surface of GaAs, the wavelength $\lambda=1.5405$ Å, for various $\langle L \rangle$ (a), σ_L (b), and σ_h (c). The miscut angle α was $0.3°$ in all cases. The distance of the lateral satellites is inversely proportional to $\langle L \rangle$ [panel (a)], their visibility depends both on σ_L and σ_h [(b) and (c)].

200, Aixtron Corp.) at a growth temperature of 560 °C and a reactor pressure of 100 mbar. The standard precursors trimethylgallium (TMGa), trimethylaluminium (TMAl), and solution trimethylindiym (TMIn, Billington Precursors) were used in combination with AsH_3 and PH_3. The strained layer superlattice (SLS) was grown onto a (100) GaAs substrate. The substrate was intentionally off-oriented toward the [110] direction and the miscut angle between the surface normal and the [100] orientation was $2.5° \pm 0.5°$. Prior to the growth of the SLS, a GaAs/(AlGa)As short period superlattice (SPS) was deposited in order to improve the surface morphology.[27,28] The layer sequence of the SLS consisted of
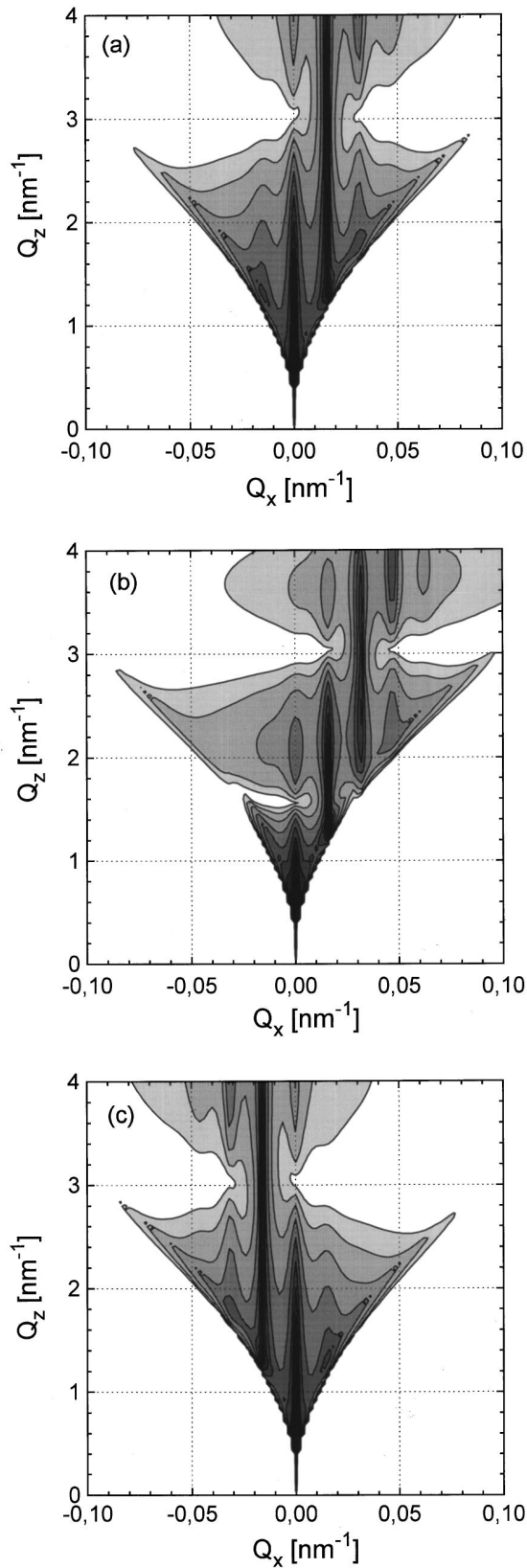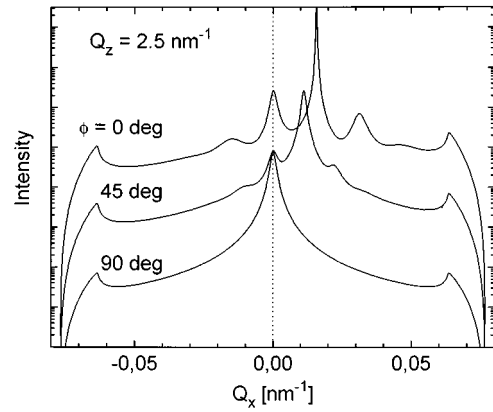
FIG. 4. The intensity $I(Q_x)$ calculated for various azimuth angles ϕ. The parameters of the surface are $\langle L \rangle = 400$ nm, $\sigma_L = 70$ nm, and $\sigma_h = 0.1$ nm. The distance of the satellites depends strongly on ϕ.

50 periods of 9.5 nm (GaIn)As/1.5 nm GaAs/9.5 nm Ga(PAs)/1.5 nm GaAs. The In and P concentrations were chosen in order to obtain a mismatch of $\pm 1\%$ for the (GaIn)As and Ga(PAs) layers, respectively. The mismatches of the two layers are of opposite signs, i.e., the layers have compressive and tensile strains (symmetrically strained layers), and consequently a zero net strain for the whole SLS occurs. The GaAs interlayers between the ternary layers are deposited in order to avoid problems associated with the strained interfaces.[27,28]

High-resolution x-ray diffraction measurements and reciprocal space mappings were performed in order to analyze the structural quality and the strain status of the SLS. No strain relaxation could be observed in the investigated sample and an excellent structural quality was confirmed.[28,29]

The x-ray specular and nonspecular reflectivity measurements were performed using a modified Philips-1880 diffractometer equipped with a 3 kW generator and a Cu target (Cu$K\alpha_1$ radiation). The equipment allows a coupled and decoupled $\omega/2\theta$ movement of the sample (ω) and the detector (2θ). The angular resolution of the sample and the detector movements is $0.0025°$. A $1/30°$ slit in front of the sample was used for the x-ray beam collimation. A post-sample Soller slit collimator ($0.057°$) and a flat graphite monochromator were used in order to obtain a sufficient high angular resolution and a reduction of the background intensity, respectively. The reflected x-ray beam intensity was measured by a proportional counter.

Numerical simulations confirmed that the reflectivity signal came mainly from the SLS interfaces; the reflectivity of the SPS lying below was suppressed due to absorption.

V. DISCUSSION

From the theoretical analysis it follows that the asymmetry of the measured ω scans for the azimuth $\phi = 0$ (Fig. 5) is caused by the terraced structure. In the angular scale used in Fig. 5, the maximum of the envelope function of the lateral satellites is for $\theta_1 - 2\theta/2 = \alpha$, where θ_1 is the incidence angle of the primary radiation and $2\theta = \theta_1 + \theta_2$ is the angle between the primary beam and the beam going through the detector slit kept constant during the ω scan (θ_2 is the angle
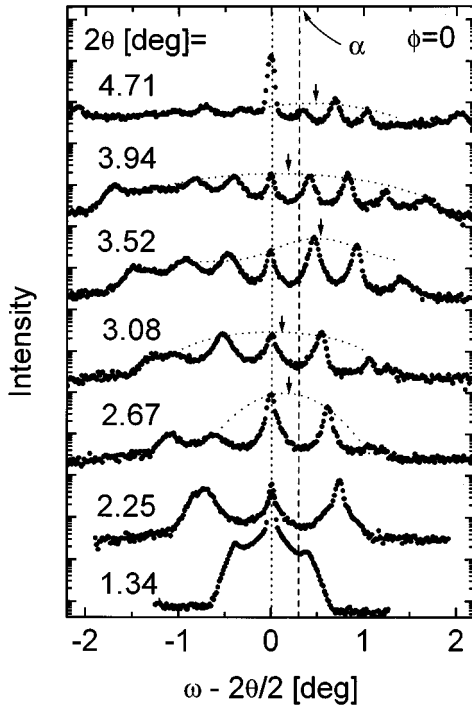

FIG. 3. The reciprocal space distribution of the intensity diffusely scattered from a terraced GaAs surface calculated for three different values of α and ϕ: (a) $\alpha = 0.3°$, $\phi = 0$, (b) $\alpha = 0.6°$, $\phi = 0$, and (c) $\alpha = 0.3°$, $\phi = 180°$. The values of the other parameters are $\langle L \rangle = 400$ nm, $\sigma_L = 70$ nm, $\sigma_h = 0.1$ nm. In reciprocal plane, the intensity maxima of the lateral satellites lie along a line inclined by the angle α from the Q_z axis.

FIG. 5. The ω scans (points) of the sample (GaIn)As/GaAs/Ga(PAs)/GaAs measured with the azimuth $\phi=0$ for various 2θ. On the horizontal axis the angle $\omega-2\theta/2$ is plotted, i.e., the angle between the wave-vector transfer $\mathbf{Q}$ and the Q_z axis. The envelope curves of the lateral satellites are plotted by the dotted lines, their maxima are denoted by short arrows. There is no distinct dependence of the position of these maxima on 2θ, their mean position is represented by the vertical dashed line.
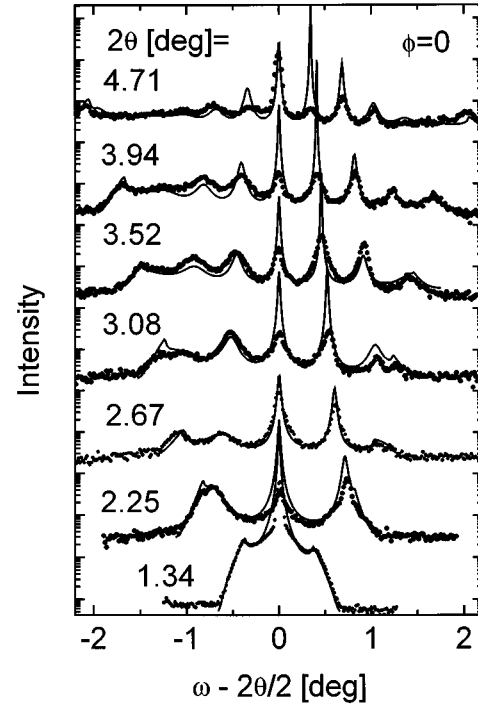

FIG. 6. The same situation as in Fig. 5, the full lines are the simulated curves (see text). A good correspondence of the measured data with the theoretical ones could be found for smaller 2θ values.

of exit). The envelope functions for various 2θ are denoted by the dotted lines in Fig. 5, their maxima by short arrows. There is no distinct dependence of the position of these maxima on 2θ; the mean position gives the value $\alpha=(0.3\pm0.1)°$.

From the distance of the lateral satellites in Fig. 5 we determined the mean terrace width $\langle L\rangle=(314\pm5)$ nm. This value and the α determined from the envelope curves have been used in the simulations of the omega scans plotted in Figs. 6, 7, and 8 for various 2θ and various azimuths ϕ. We used formulas (22) and (23) for the calculation of the scattered intensity, the pair correlation function was assumed in the form (8), taking into account the gamma distribution (9) of the terrace widths and lengths. We transformed the (Q_x,Q_z) dependence of the scattered intensity (23) into the angular (θ_1,θ_2) dependence using the transformation formulas

$$Q_x=K(\cos\theta_2-\cos\theta_1), \quad Q_z=K(\sin\theta_2+\sin\theta_1). \quad (24)$$

From the comparison of the measured and calculated scans for $\phi=0$ (Fig. 6) we determined the remaining parameters of the terrace structure. Since the parameters σ_L and σ_h are correlated, it is not possible to determine both of them from the same measurement. Therefore, we have assumed $\sigma_h=0$ and then we found $\sigma_L=(50\pm10)$ nm.

The vertical correlation of the interface profiles has nearly no influence on the ω scans. Therefore, the values of χ and

$\Lambda_\perp$ could be chosen arbitrarily. From the high-resolution diffractometry we determined $\chi=(42\pm2)°$ (this will be the subject of the next paper) and we set $\Lambda_\perp=100$ nm.
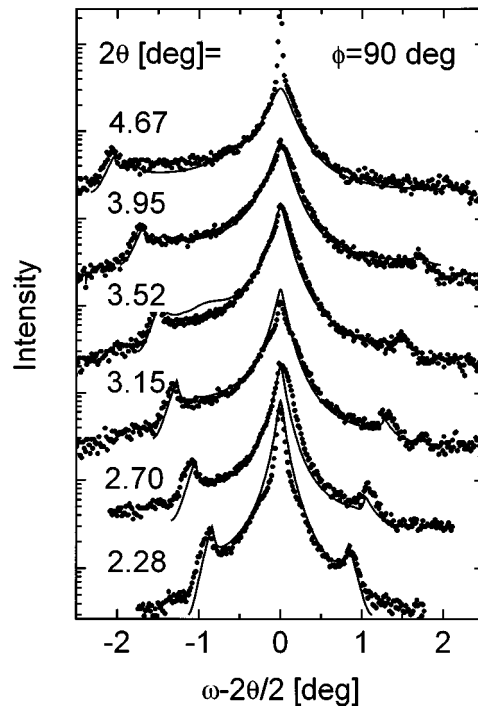
The coincidence of the theoretical and experimental

FIG. 7. The measured (points) and calculated (lines) ω scans for the azimuth angle $\phi=90°$. No lateral satellites are visible, since the scattering plane is oriented along the staircase steps, i.e., the x axis lying in the scattering plane is parallel to the axis x_2 — see Fig. 1.
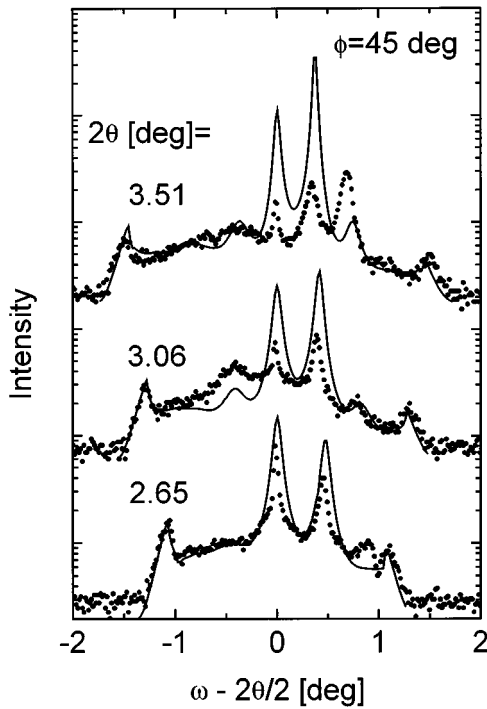
FIG. 8. The same as Fig. 7, but with the azimuth angle $\phi=45°$. A good agreement of the measured and calculated curves was achieved only for the smallest value of 2θ.

curves is better for smaller 2θ. For larger 2θ, the measured satellites are lower than the calculated ones while their widths agree. This could be caused by usual roughness superimposed to the terrace structure. This roughness gives rise to an additional diffuse scattering that increases the background of the measured ω scan, and, consequently, relatively decreases the satellites without their broadening.

The omega scans measured in the azimuth $\phi=90°$ (Fig. 7) do not depend on the terrace widths L. From the comparison with the theoretical curves we found the mean terrace length $\langle D \rangle =(1.0\pm0.2)$ μm. The subsidiary maxima on those curves are so-called Yoneda peaks,[1] i.e., they lie in points, where θ_1 or θ_2 equal the critical angle θ_c of total external reflection. There are no lateral satellites on those curves, therefore the distribution of the terrace lengths is exponential ($M'=1$) with the dispersion $\sigma_D^2=\langle D \rangle^2=1$ μm^2. This interpretation of the ω scans measured for $\phi=90°$ is not unique; the same results can be obtained assuming a fractal roughness[1] with the fractal exponent $h=1/2$ (i.e., the fractal dimension 2.5) and the correlation length $\langle D \rangle$.

Using the above values of the parameters we simulated the omega scans for the azimuth $\phi=45°$ and compared them with the experiments (Fig. 8). The main features of the experimental scans are properly reproduced — the distance of the satellites is smaller and the satellites are broader than those for $\phi=0$. Similarly to $\phi=0$, the agreement of the measured and calculated scans is better for smaller 2θ.

The value of α does not agree with the miscut angle $\alpha_M=(2.5\pm0.1)°$. A possible explanation of this fact follows from Fig. 9. The interface consists of monolayer steps of the height $h_0\approx2.83$ Å bunched into larger steps having the mean width $\langle L \rangle =314$ nm. These large steps are composed of
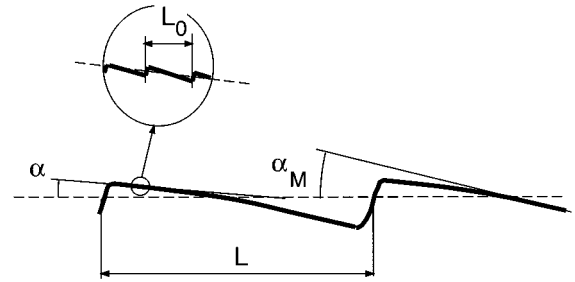

FIG. 9. Probable structure of the terraced interface. The angle α between the terrace levels and the mean interface is smaller than the miscut angle α_M. The terrace levels consist of small monolayer terraces of the width L_0 making the nominal miscut angle α_M with the mean interface. Due to the inhomogeneous distribution of these terraces, the large terrace levels are not exactly flat.

$\alpha\langle L \rangle /h_0\approx50$ monolayer steps. However, some monolayer steps are distributed in the terraces, too, so that the terrace levels are no longer parallel to (001) planes. Similar structure has been postulated previously.[17] As shown in Fig. 9, these large terraces consist of a sequence of small (001) terraces divided by monolayer steps h_0. These terraces make the true miscut angle α_M with the mean surface. Their mean width can be estimated using the simple formula

$$\langle L_0 \rangle \approx \frac{h_0}{\alpha_M-\alpha} \qquad (25)$$

that gives approximately 74 Å.

Using the theory outlined above, we find that such an interface structure should produce an additional maximum of the diffuse scattering intensity inclined in reciprocal plane by the angle α_M to the Q_z axis. In order to verify this interpretation, it was necessary to measure an ω scan with 2θ larger than $2\alpha_M$. Since the miscut value α_M of the sample studied above was rather large, this ω scan would be very weak. Therefore, we have measured the ω scans of another sample (sample B), having the same structure of the previous one,
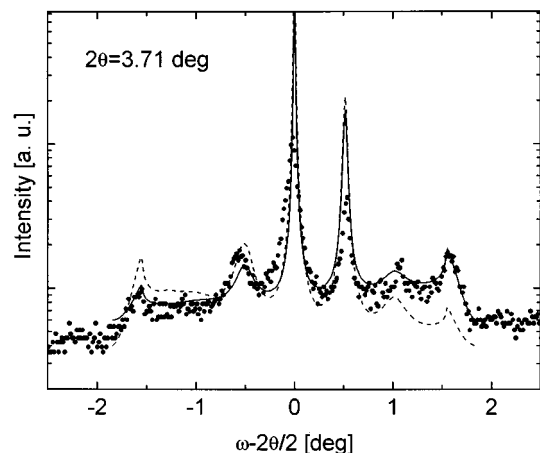

FIG. 10. The ω scan (points) of sample B measured for $2\theta=3.71°$. The full (dashed) lines represent the simulations performed with (without) the monolayer terraces, respectively. The presence of the monolayer terraces explains the asymmetry of the measured scan.

but with the miscut angle of the GaAs substrate smaller $[\alpha_M^B=(1.5\pm0.1)°]$. In the azimuth $\phi=0$ (Fig. 10) the ω scans measured for larger 2θ exhibited a significant asymmetry of the intensity distribution between the lateral satellites. This asymmetry cannot be caused by the changes in the irradiated surface area of the sample (this would give rise to the opposite asymmetry). Our explanation is that this asymmetry is due to the diffuse scattering from the monolayer terraces. Since the mean width of these terraces is too small and/or their width dispersion is too large, we cannot detect their nonzero lateral satellites.

In Fig. 10 we compared the measured ω scan of sample B with the simulations performed without (dashed) and with (full line) the monolayer terraces. For their mean width we used the value $\langle L_0 \rangle=130$ Å following from Eq. (25) and from the values of α and α_M for this sample, and we assumed that the order of their gamma distribution is $M_0=1$. The monolayer terraces explain well the measured asymmetry.

VI. CONCLUSIONS

On the basis of the statistical description of a terraced interface we calculated the diffuse x-ray reflectivity of a single-crystalline multilayer grown on a misoriented substrate. We compared the theoretical results with the measurements performed on an $In_xGa_{1-x}As/Ga_{1-x}As_xP/GaAs$ superlattice. From the comparison we determined the size of the terraced interface and the orientation of the terrace levels with respect to the crystallographic (001) planes.

ACKNOWLEDGMENTS

[1] S. K. Sinha, E. B. Sirota, S. Garoff, and H. B. Stanley, Phys. Rev. B **38**, 2297 (1988).

[2] V. Holý, J. Kuběna, I. Ohlídal, K. Lischka, and W. Plotz, Phys. Rev. B **47**, 15 896 (1993).

[3] V. Holý and T. Baumbach, Phys. Rev. B **49**, 10 688 (1994).

[4] T. Salditt, T. H. Metzger, and J. Peisl, Phys. Rev. Lett. **73**, 2228 (1994)

[5] V. M. Kaganer, S. A. Stepanov, and R. Köhler, Phys. Rev. B **52**, 16 369 (1995).

[6] J. Krim and G. Palasantzas, Int. J. Mod. Phys. B **9**, 599 (1995).

[7] D. K. G. de Boer, Phys. Rev. B **53**, 6048 (1996).

[8] T. Salditt, D. Lott, T. H. Metzger, J. Peisl, G. Vignaud, P. Høghøj, O. Schärpf, P. Hinze, and R. Lauer, Phys. Rev. B **54**, 5860 (1996).

[9] V. F. Sears, Phys. Rev. B **48**, 17 477 (1993).

[10] S. F. Edwards and D. R. Wilkinson, Proc. R. Soc. London, Ser. A **381**, 17 (1982).

[11] M. Kardar, G. Parisi, and Y. C. Zhang, Phys. Rev. Lett. **56**, 869 (1986).

[12] S. K. Sinha, M. K. Sanyal, S. K. Satija, C. F. Majkrzak, D. A. Neumannn, H. Homma, S. Szpala, A. Gibaud, and H. Morkoc, Physica B **198**, 72 (1994).

[13] S. K. Sinha, J. Phys. III France **4**, 1543 (1994).

[14] E. A. Kondrashkina, S. A. Stepanov, R. Opitz, M. Schmidbauer, and R. Köhler, in *17th Congress IUCr, Collected Abstracts, Seattle, 1996*, edited by J. F. Griffin (International Union of Crystallography, Seattle, 1996), p. C-474.

[15] R. L. Headrick and J.-M. Baribeau, J. Vac. Sci. Technol. B **11**, 1514 (1993).

[16] R.L. Headrick and J.-M. Baribeau, Phys. Rev. B **48**, 9174 (1993).

[17] Y. H. Phang, C. Teichert, M. G. Lagally, L. J. Peticolos, J. C. Bean, and E. Kasper, Phys. Rev. B **50**, 14 435 (1994).

[18] R. L. Headrick, J.-M. Baribeau, and Y. E. Strausser, Appl. Phys. Lett. **66**, 96 (1995).

[19] J.-M. Baribeau and D.J. Lockwood, J. Electron. Mater. **24**, 341 (1995).

[20] P. M. Reimer, Y. Yamaguchi, J. H. Li, and H. Hashizume (Ref. 14), p. C-473.

[21] Q. Shen, J. P. Chang, G. Navrotski, and J. M. Blakely, Phys. Rev. Lett. **64**, 451 (1990).

[22] S. Pflanz, H. L. Meyerheim, W. Moritz, I. K. Robinson, H. Hoernis, and E. H. Conrad, Phys. Rev. B **52**, 2914 (1995).

[23] I. K. Robinson, K. L. Whiteaker, and D. A. Walko, Physica B **221**, 70 (1996).

[24] R. Pynn and S. Baker, Physica B **198**, 1 (1994).

[25] P. R. Pukite, C. S. Lent, and P. I. Cohen, Surf. Sci. **161**, 39 (1985).

[26] Z. H. Ming, A. Krol, Y. L. Soo, Y. H. Kao, J. S. Park, and K. L. Wang, Phys. Rev. B **47**, 16 373 (1993).

[27] S. Lutgen, T. Marschner, T. F. Albrecht, W. Stolz, E. O. Göbel, and L. Tapfer, Mater. Sci. Eng. **B21**, 249 (1993).

[28] T. Marschner, L. Tapfer, N. Y. Jin-Phillipp, F. Phillipp, S. Lutgen, M. Volk, W. Stolz, and E. O. Göbel, Solid State Electron. **40**, 819 (1996).

[29] C. Giannini, L. Tapfer, Y. Zhuang, L. De Caro, T. Marschner, and W. Stolz (unpublished).